

Infrared Spectroscopic Studies of Carbon Monoxide Adsorbed on a Series of Silica-Supported Copper Catalysts in Different Oxidation States

M. A. KOHLER,* N. W. CANT,¹ M. S. WAINWRIGHT,* AND D. L. TRIMM*

*School of Chemistry, Macquarie University, North Ryde, New South Wales 2109, Australia, and *School of Chemical Engineering and Industrial Chemistry, University of New South Wales, P.O. Box 1, Kensington, New South Wales 2033, Australia*

Received January 4, 1988; revised December 7, 1988

Infrared spectroscopy has been used to study the adsorption of carbon monoxide (358–493 K, 0.1–20 kPa) on four copper-on-silica (2–10 wt% Cu) catalysts prepared by the "ion-exchange" technique. The measurements are made for each sample in three different states: unreduced (predominantly Cu²⁺), reduced (Cu⁰), and partially reoxidised in nitrous oxide (Cu⁺). On unreduced samples, a major absorption band between 2127 and 2132 cm⁻¹ due to CO adsorbed on small CuO particles and a weak band at 2199 cm⁻¹ due to CO on isolated Cu²⁺ ions incorporated in the silica surface have been identified. The former adsorption obeys a Langmuir isotherm with a heat of adsorption of 29 kJ/mol independent of CuO particle size and surface coverage. After catalyst reduction, the major absorption band lies between 2090 and 2113 cm⁻¹ and arises from CO linearly bound to very small (1- to 5-nm) copper metal clusters. The observed frequency shifts indicate the presence of steps and terraces similar to low index Cu planes in very small particles (1- to 2-nm), and the presence of similar higher index Cu planes on larger clusters (2- to 5-nm). The absorption is described by a Freundlich isotherm with the heat of CO adsorption decreasing with coverage from 50 to 22 kJ/mol on bigger particles but more constant (27 to 22 kJ/mol) on small particles. A surface copper/CO atomic ratio increasing from 5 to 12 is established at equilibrium saturation between 358 and 493 K using extinction coefficients determined in this study. In the reduced catalyst, a weakly adsorbed ($\Delta H_a = -20$ kJ/mol) species assigned to CO bound to isolated Cu⁺ ions is also found and absorbs at 2175 cm⁻¹. The frequency of this band does not vary with catalyst loading and is not affected by reoxidation of the catalyst in nitrous oxide. © 1989 Academic Press, Inc.

INTRODUCTION

The performance of a heterogeneous catalyst is dictated by events at the gas–solid interface. Activity and selectivity depend on the nature and amount of adsorbed species and the effect of the geometric and electronic structure of the catalyst on adsorption. As a result, there is considerable interest in the characterisation of the catalyst surface and of species adsorbed thereon. Of the many techniques that have been applied to gas–solid systems, infrared spectroscopy is both sensitive and particularly informative. Thus, for example, the vibrational spectra of carbon monoxide

(CO) adsorbed on platinum (1), nickel (1, 2), platinum/ruthenium (3), and copper (4–6) have revealed much information about the adsorbed gas and the structure of the surface on which it is adsorbed. In some cases, it has been found possible to apply the technique to catalysts under reaction conditions (3, 7), thereby providing extra information on adsorbed species involved in a reaction.

The adsorption of CO on metals with filled *d* shells, such as copper, silver, and gold, is much weaker than that on other metals that can form bulk carbonyls. As a result, differences in surface structure do not lead to infrared absorption bands as well-resolved as those with transition metals. However, the extensive work by

¹ To whom correspondence should be addressed.

Pritchard and co-workers (8–11) on single-crystal copper indicates a significant correlation between the position of the absorption maxima attributed to CO and the surface structure of the metal. Furthermore, substantial changes in the characteristic wavenumber and intensity of the CO absorption bands have been observed when changing the chemical state of the copper from supported copper oxide (4, 5, 12, 13) to copper metal particles (4–6, 14).

Copper-on-silica catalysts prepared by the ion-exchange method have been the subject of recent interest (15). Detailed studies of the preparation (15) and characterization (16) of the catalysts revealed the existence of two copper species present on calcined (773 K in air) samples:

(a) Isolated Cu²⁺ ions incorporated in the silica surface by ion exchange of one Cu²⁺ ion with two silanol surface groups. For catalysts containing 2–9 wt% Cu, these ion-exchanged species represent 0.5 to 0.8 wt% Cu or 10–25% of the total Cu content and occupy 15 to 20% of the available silanol groups (15). Upon reduction, only Cu⁺ was produced and no change in distribution was observed.

(b) CuO particles, originally precipitated as Cu(OH)₂ during preparation and oxidised during calcination. The particles are distributed irregularly on the silica surface and are of flat disk to semispherical shape. Their mean diameters vary from 1.5 nm (2.1 wt% Cu) to 5 nm (9.5 wt% Cu) (16). They are fully reduced to copper with minimal interparticle migration and agglomeration. However, as expected from the small anisotropy of the surface energy of copper (17, 18), the reduced particles tend to a spherical shape of diameter ranging from 1 nm (2.1 wt% Cu) to 3 nm (9.5 wt% Cu) (16). The resulting dispersion of copper is much higher than that observed in Cu/SiO₂ prepared by other techniques (6, 12, 19).

On the basis of this detailed knowledge of the copper structure, the present studies were intended to investigate the adsorption

of carbon monoxide on copper ion-exchanged on silica, using infrared spectroscopy as the main characterisation technique. Attention was focused on the four samples that had been the subject of previous investigation (2.1, 4.1, 5.9, and 9.5 wt% Cu loading) (15, 16) in the calcined, reduced, and reoxidised/reduced states.

EXPERIMENTAL

The copper-on-silica catalysts were prepared by ion exchange of an Aerosil-type silica (Aerosil 200, Degussa AG) following the procedure described in detail elsewhere (15). Four different samples containing 2.1, 4.1, 5.9, and 9.5 wt% copper were selected as a result of the fact that detailed characterisation of these samples has been reported (16). Blank experiments were carried out using a sample of the support material which had been subjected to a treatment similar to that used in the catalyst preparation but omitting copper. Samples of each catalyst were finely ground and pressed into 3.2-cm-diameter pellets by applying 60 MPa for 5 min. Disks of 1.9 cm diameter weighing 70 mg (high loadings) to 90 mg (low loadings) were cut from each pellet.

The infrared cell/flow reactor was identical to that described by Monti *et al.* (7). The optical path length between the windows was 2.4 mm, which kept the absorbance due to gas phase CO below 0.025 with the catalyst disk in place. The temperature of the cell was maintained to within 1 K of a preset value by a temperature controller connected to the thermocouple located inside the reactor. The cell/reactor was connected to a supply system comprising calibrated Brooks flow sensors for high-purity He, H₂, and a 20.2% CO/H₂ gas mixture (CIG, Australia) and a rotameter and needle valve for pure nitrous oxide. This arrangement allowed stable flows (10–80 ml/min) of CO in different carriers at partial pressures of up to 20 kPa.

Prior to the study on unreduced catalysts, adsorbed water was removed by flow-

ing helium (40 ml/min) at 453 K over the catalyst discs for 30 min and helium was then used as the main carrier throughout this part of the investigation. No reduction of the catalyst samples by the CO/H₂ mixture was detected below 450 K except for the 9.5 wt% sample, where slow and partial reduction started at approximately 430 K. As a result, the low-temperature adsorptions were measured first in this part of the investigation. Reduction of the catalysts was carried out *in situ* with flowing hydrogen at 543 K, initially using a 10% H₂/He mixture (40 ml/min) and completing the reduction in pure hydrogen overnight. No difference in the adsorption behavior was identified when reducing for 2 h at 543 K only. Hydrogen was used as carrier on reduced samples and the order of the measurements was stochastic over the temperature and CO partial pressure ranges. Reoxidation of the samples by N₂O was carried out starting at 363 K under increasing partial pressures (10 to 50% in He) and completed at 523 K for 2 h in pure N₂O.

Infrared spectra were recorded with a Perkin-Elmer Model 580 ratio-recording spectrometer linked to a Model 3600 infrared data station which enabled the acquisition and storage of digitized spectra and data processing. Background spectra corresponding to cell plus flow streams at various compositions plus support (SiO₂) disk were stored. Subtraction of these using appropriate multiplication factors, from spectra corresponding to the Cu/SiO₂ samples in the presence of CO, then revealed the features due to species adsorbed on copper alone. With appropriate scaling and smoothing, bands with absorbances of 0.01 or less could be investigated with considerable confidence. The catalyst samples had a maximum transmission of 30 to 35% in the most important 2200 to 2100 cm⁻¹ region, but all spectra were recorded between 4000 and 1300 cm⁻¹. Transmission was limited by the strong absorption of the silica at the low end of this frequency range.

Carbon monoxide adsorption isotherms

on Cu²⁺, Cu⁰, and Cu⁺ were also established separately in a standard glass adsorption system. A 0.45-g sample of the 5.9 wt% Cu was reduced or reoxidised *in situ* by circulating H₂ or N₂O, respectively.

RESULTS AND DISCUSSION

1. CO Adsorption on Unreduced Catalysts

All unreduced catalyst samples investigated at 358, 378, and 414 K showed one major absorption band due to adsorbed carbon monoxide. Figure 1 displays a typical series of results for the four catalysts at almost complete coverage (>80%). The peak maxima always shifted from 2127 ± 2 cm⁻¹ at approximately 10% saturation to 2132 ± 2 cm⁻¹ at saturation but with an invariant half-width of 16 ± 1 cm⁻¹. These peak frequencies agree very closely with results for carbon monoxide adsorption on CuO surfaces as reported in the literature (4, 12, 20). However, the half-width of the bands is only one-third the value reported for high copper loadings on silica (>15 wt%) where the particle size is much larger (12).

The results in Fig. 1 indicate a very weak

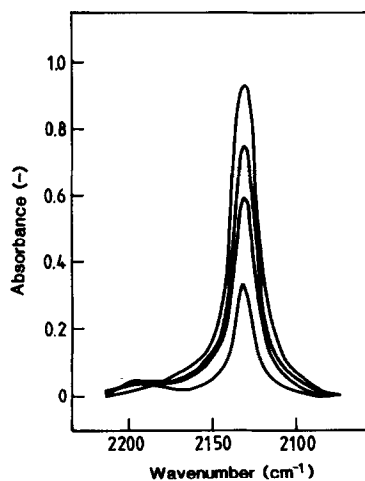


FIG. 1. Infrared spectra of CO adsorbed on unreduced Cu/SiO₂. The infrared absorption band around 2130 cm⁻¹ is attributed to CO on crystalline CuO with the catalyst loading decreasing from top to bottom (9.5, 5.9, 4.1, and 2.1 wt%). The minor band around 2199 cm⁻¹ is assigned to CO on isolated Cu²⁺ sites.

additional peak at $2199 \pm 4 \text{ cm}^{-1}$. Such high-frequency bands have been correlated with weakly held species and a similar band at 2204 cm^{-1} has been attributed to carbon monoxide adsorbed on isolated Cu^{2+} ions incorporated in the silica surface (12). This interpretation for the 2199 cm^{-1} band observed here seems reasonable given its somewhat greater intensity relative to the main peak for the samples of lower copper loadings.

A number of additional bands were observed in the 1700 to 1300 cm^{-1} region and other spectral changes were evident around 3600 to 2800 cm^{-1} when the calcined catalyst samples were exposed to carbon monoxide. Well-defined peaks were identified at 1518 and 1425 cm^{-1} with additional less-defined changes occurring at 3622 , 2920 , 1645 , and 1347 cm^{-1} . The intensity of individual bands did not exceed 0.30 in absorbance. All peaks were roughly proportional to the CO partial pressure although they persisted over a relatively long period (>30 min) during flushing in a helium stream. They completely disappeared in hydrogen within approximately 10 min at moderate temperature (403 K) during which no modification of the main absorption band near 2130 cm^{-1} was detected. These bands are characteristic of oxidative interactions of CO with CuO (4, 5) and can be attributed to bicarbonates, carbonates, and formates (21–24).

The intensities of the main absorbance (2130 cm^{-1}) may be plotted as a function of the CO partial pressure using the Langmuir isotherm approach, i.e.,

$$\frac{P}{A} = \frac{1}{A_{\infty}K} + \frac{P}{A_{\infty}}, \quad (1)$$

where P represents the CO partial pressure, K the adsorption equilibrium constant, A the actual absorbance, and A_{∞} the absorbance at saturation coverage. Typical results are shown in Fig. 2 for the data collected at 378 K .

It is clear that carbon monoxide adsorption on unreduced catalysts follows the Langmuir isotherm quite closely. Further-

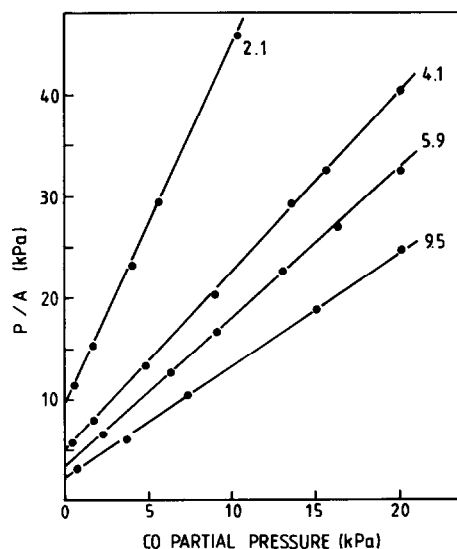


Fig. 2. Typical plot of CO adsorption data according to Eq. (1) at 378 K for the four unreduced catalysts. Cu loading (wt%) shown on the diagram.

more, plotting the data measured at other temperatures in the same way as in Fig. 2 resulted in sets of parallel lines for the individual catalysts (excluding data for the $9.5 \text{ wt}\%$ sample at 441 K , where some partial reduction was observed as reported above). In terms of Eq. (1) parallel lines translate into a saturation absorbance independent of temperature in the range of this study and these are tabulated in Table 1. These values are adjusted to take into account the difference disk weights and thus allow direct comparison between catalyst samples. The value of A_{∞} is linear with copper loading (correlation coefficient >0.995). Very similar values for the adsorption equilibrium constant K were obtained for all catalysts using A_{∞} in Table 1 and intercepts from Fig. 2 as shown in the final column of Table 1. An approximate heat of adsorption of 25 kJ/mol is identified by the application of the van't Hoff equation to the average K values listed in Table 1.

On the basis of the adsorption isotherms described above, it was also possible to construct isosteres for the four catalyst samples over the pressure range 0.2 to 20

TABLE 1

Normalised Absorbance and Adsorption Equilibrium Constants for Carbon Monoxide Adsorbed on Unreduced Cu/SiO₂ as a Function of Temperature

Temperature (K)	A _∞ (cm ² /g) at various Cu loadings				10 ⁴ × K (Pa ⁻¹)
	2.1 wt%	4.1 wt%	5.9 wt%	9.5 wt%	
358	9.1	18.9	26.1	30.2	7.9 ± 0.7
378	9.2	18.6	25.3	31.5	3.2 ± 0.5
441	9.2	18.3	25.7	31.6	1.8 ± 0.3

kPa as a function of surface coverage ($\theta = A/A_{\infty}$); a typical example is shown in Fig. 3. A constant heat of adsorption of 29 ± 2 kJ/mol was calculated for the adsorption of CO on Cu²⁺ independent of surface coverage (between 0.1 and 0.9) and for all catalyst samples except the 9.5 wt% sample at low coverage (<0.5). In the latter case, a slight increase of the heat of adsorption (approximately 5 kJ/mol) was observed when θ approached 0.1. No comparable data for the heat of adsorption on a similar Cu²⁺ system were found in the literature. Nevertheless, the values seem relatively small with respect to CO adsorption on copper metal, where values up to ca. 60 kJ/mol have been measured (7, 14, 36). However, the measured heat of adsorption agrees closely with the value of 21.7 kJ/mol reported by London and Bell (5) for CO adsorption on supported Cu⁺.

2. CO Adsorption on Cu/SiO₂: Major Peak

Background spectra following reduction in hydrogen alone showed differences in the OH stretching region 3600 to 3200 cm⁻¹ relative to unreduced samples. Absorbances were increased by 10 to 20% over the region for all catalyst samples, and this can be explained by the increased exposure of silanol groups due to the decrease in size of copper particles, compared to their CuO precursors, upon reduction (16, 24). This effect was slightly more pronounced in the case of high copper loadings

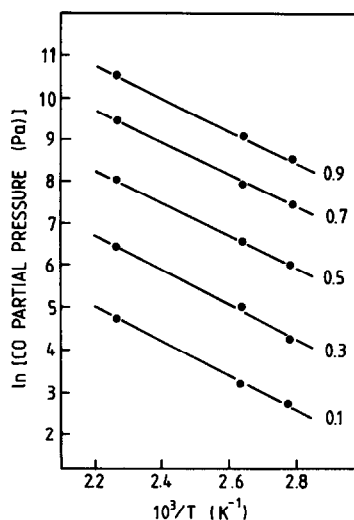


FIG. 3. Adsorption isosteres for CO on unreduced catalysts at various surface coverages ($\theta = A/A_{\infty}$) typically represented by the results for a 5.9 wt% sample.

(larger particles which expose more silanol sites when shrinking) as expected from the XPS/AES/TEM results on these samples (16). Small modifications to the spectra also took place between 1650 and 1400 cm⁻¹, and are most probably connected to the same phenomenon (24).

Infrared spectra recorded in the presence of carbon monoxide were quite different from those for the unreduced samples. After subtraction of the reduced sample background, no evidence of any formate or carbonate species was detected. Two main features due to adsorbed CO were identified between 2050 and 2200 cm⁻¹; they are shown for near-saturation conditions (>0.9) over the series of catalysts in Fig. 4.

The major absorption band is characterised by a maximum, which shifts steadily between 2090 and 2113 cm⁻¹ with both surface coverage and catalyst copper loading (as shown in Table 2), together with a slight asymmetry towards lower frequencies (Fig. 4). At constant coverage no significant effect of temperature was detected in the range used in this study. These absorption bands are typical for carbon monoxide adsorption on metallic copper (6, 9, 14).

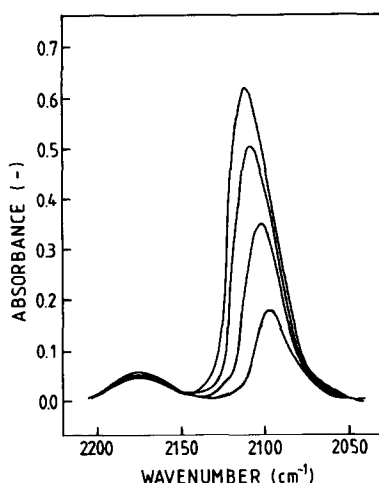


FIG. 4. Infrared spectra of CO adsorbed on reduced catalysts at 20 kPa partial pressure. The main infrared absorption band around 2098 to 2113 cm^{-1} is assigned to CO on small metal particles with the catalyst loading decreasing from top to bottom (9.5, 5.9, 4.1, and 2.1 wt%). The minor band around 2175 cm^{-1} is attributed to CO adsorbed on isolated Cu^+ sites.

Shifts towards higher frequencies with increasing surface coverage are well documented. On extended single crystal surfaces a shift of typically 9 cm^{-1} has been found (8, 10) and a similar shift has been identified on supported catalysts (9, 14). The shift has been correlated with the variation of the surface potential with coverage, which is usually found to increase with coverage in the initial stages but to pass through a maximum and to decrease on saturation (9). As in this study, the frequency shift occurs close to saturation, where LEED results indicate a compression from an ordered adsorption structure to an out-of-registry structure (11, 25). The shift to higher wavenumber has then been related to vibrational dipole-dipole coupling of adsorbed CO molecules, which is intensified at higher surface coverages (26). By application of the isotopic dilution method, substantial shifts of up to 40 cm^{-1} have been identified on low index Pt and Pd single-crystal surfaces (27, 28). Given the much less complete equilibrium surface cover-

ages of CO/Cu, however, the coupling effect would be expected to be much lower on copper or copper oxide surfaces (29).

Support effects in the infrared spectra of chemisorbed carbon monoxide are well known (24), although they have been found to be negligible on SiO₂ supports (29). Nevertheless, the observed peak maxima in the present system also vary considerably with different preparations which produce different copper dispersions. The frequencies observed during the present study are significantly lower than those observed on high weight percent Cu/SiO₂ catalysts (2104 to 2139 cm^{-1} (6)) but are similar to those reported by other authors for lower content Cu/SiO₂ (5–15 wt%) (2100 cm^{-1} (14), 2103 and 2105 cm^{-1} (9), and 2110 cm^{-1} (30)). Major bands with frequencies below 2100 cm^{-1} have been identified for supported copper catalysts only in the case of magnesia (2081 cm^{-1} (9)). It appears then that the frequencies below 2100 cm^{-1} observed in this investigation are a result of the extremely high copper dispersion on the present Cu/SiO₂ catalysts. A similar particle size effect has also been established for supported nickel catalysts (31, 32).

For the closely packed (111), (110), and (100) planes of copper, Pritchard *et al.* (9) recorded absorbance maxima at 2075 to 2095 cm^{-1} for CO adsorption at 77 K. The main maxima for stepped surfaces (211), (311), and (755) were between 2095 and 2110 cm^{-1} . These single-crystal results

TABLE 2

Peak Frequencies as a Function of Coverage ($\theta = A/A_s$) and Average Half-Width for Carbon Monoxide Adsorption on Copper Particles in Reduced Cu/SiO₂ Samples

Cu loading (wt%)	Frequency (cm^{-1}) at various surface coverages (θ)					Half-width (cm^{-1})
	0.1	0.3	0.5	0.7	0.9	
2.1	2090	2091	2094	2097	2098	24
4.1	2098	2100	2101	2104	2104	26
5.9	2103	2103	2105	2109	2110	29
9.5	2104	2105	2107	2112	2113	30

point directly to the presence of low-index contributions to the supported copper surfaces in the present study. Given the asymmetry of the absorption bands, this effect appears to be always present but dominates at low copper loadings (Fig. 4). Thus, at a catalyst loading of 2.1 wt%, an approximate mean copper spherical particle size of 1 nm has been established (16). Terraces similar to a (111) structure and steps similar to a (100) structure are expected to dominate on the outer surface of these copper metal particles (12, 17), and the observed absorption frequencies between 2090 and 2098 cm^{-1} (Table 2) are typical of such structures (9). Increasing the mean particle diameter to about 1.5 nm (4.1 wt% sample (16)) is believed to change this structure only slightly (18) and the observed frequencies change little (Table 2). On the other hand, particles of up to 5 nm diameter have been identified on reduced catalyst at the two higher loadings, and these particles are most probably approximated by the stepped surfaces (211), (311), and (755) (12). The density of these steps is believed to prevent adsorption of CO in the ordered structure mentioned above (6, 11) which in turn leads to the higher frequencies for adsorbed CO observed in this investigation.

The significant asymmetry of the CO absorption bands towards frequencies around 2070 cm^{-1} (Fig. 4) is therefore most probably assignable to contributions of closely packed copper atoms on the particle surfaces which are similar to low-index single-crystal faces. Larger particles still may be expected to result in substantially higher frequencies such as 2146 cm^{-1} observed on particles of up to 500 nm diameter and reported by other authors (6). Thus, the typical half-widths of the spectra, which increase slightly with copper loading (Table 2), are probably connected to the increasing heterogeneity of the copper particle sizes on these catalysts (16).

The relation between amount adsorbed and intensity of the absorption bands was tested for conformity to Eq. (1). For all cat-

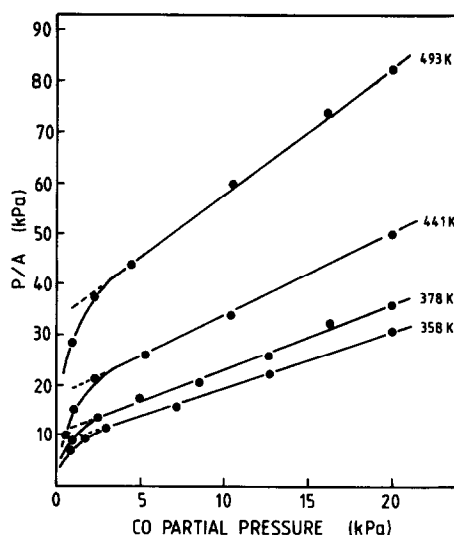


FIG. 5. CO adsorption data for metallic copper on a reduced 9.5 wt% sample (2104–2113 cm^{-1} band, Table 2) at various temperatures when plotted according to Eq. (1). The deviations from a Langmuir isotherm occur below 2.5 kPa CO partial pressure.

alysts, adsorption behaviour according to the Langmuir isotherm was found between 2 and 20 kPa CO partial pressure at all temperatures investigated (i.e., 358, 378, 441, and 493 K). However, below approximately 2 kPa, substantial deviations from this model were identified and the deviation increased at higher copper loadings (Fig. 5). The slopes of the isotherms, and thus the inferred saturation coverage, were found to vary quite substantially with temperature, as listed in Table 3 (after incorporating the specific disk weights and normalizing to a constant peak half-width of 25 cm^{-1}). This is not surprising given the substantial fall in the equilibrium saturation adsorption of carbon monoxide on Raney copper over the range 77 to 363 K (33). On the other hand, at fixed temperature values of A_{∞} normalised by the specific copper surface areas (A_{∞}^s in Table 3) showed no significant dependence on metal loading (and hence mean copper particle size).

It was then possible to establish the isotherms for CO adsorption on metallic copper

TABLE 3

Peak Absorbance for Carbon Monoxide Adsorption on the Copper Particles Present in Reduced Cu/SiO₂ Normalised for Disk Weight, A_{∞} (in cm²/g), and for Copper Metal Area, A_{∞}^s (cm²/m²(Cu))^a

Temperature (K)	A_{∞} and A_{∞}^s at various Cu loadings							
	2.1 wt%		4.1 wt%		5.9 wt%		9.5 wt%	
	A_{∞}	A_{∞}^s	A_{∞}	A_{∞}^s	A_{∞}	A_{∞}^s	A_{∞}	A_{∞}^s
358	7.4	1.54	14.2	1.49	23.7	1.60	30.6	1.57
378	6.7	1.39	12.8	1.35	18.9	1.30	26.5	1.36
441	5.0	1.04	9.7	1.02	13.9	0.97	21.3	1.08
493	3.6	0.75	6.4	0.68	10.4	0.72	15.0	0.75

^a A_{∞}^s is A_{∞} (cm²/g) divided by copper metal area (m²(Cu)/g).

at constant absorbance. Given the apparent variation of A_{∞} with temperature, the surface coverage was related to A_{∞} at 358 K, i.e., $\theta = A/A_{\infty 358}$. Data for the 4.1% copper catalyst are shown in Fig. 6. The isosteres are close to parallel and the heats of adsorption calculated from the slopes of these plots show only a small decline with coverage as shown in Fig. 6. The 2.1% sample showed even less variation. However, the 5.9% and 9.5% samples have distinctly higher heats of adsorption at low coverages

and this accounts for deviation from Langmuir behaviour in the plots of Fig. 5.

It is clear from these results that carbon monoxide adsorption on the reduced Cu/SiO₂ catalysts can be approximated by the Langmuir isotherm over almost the entire range of partial pressures (>0.2 kPa) of this study for low copper contents and above 2.5 kPa (or surface coverages >0.3, respectively) for substantial copper loadings. Below these limits, a considerable increase in heat of adsorption is observed which, in turn, explains the susceptibility of this type of catalyst to inhibition by modest pressures of carbon monoxide (7, 34).

The measured heats of adsorption are towards the low end of the values reported in the literature, which lie between approximately 20 and 70 kJ/mol (5, 7, 9, 14). Higher values generally dominate at surface coverages below 0.1 (35, 36). Decreasing heat of CO adsorption with increasing coverage is well known and has been identified on copper single-crystal surfaces such as Cu (311) (from 61 kJ/mol at $\theta = 0$ to 22 kJ/mol at $\theta = 1$ (36)). The observed decrease was S-shaped with the steepest fall in the heat of adsorption occurring when the surface potential was at its maximum (θ ca. 0.5). From this result, it is seen that the copper particles on a high-loading Cu/SiO₂ catalyst are again very similar to a high-index Cu single-crystal surface such as (311). The steady decrease of the measured heats of adsorp-

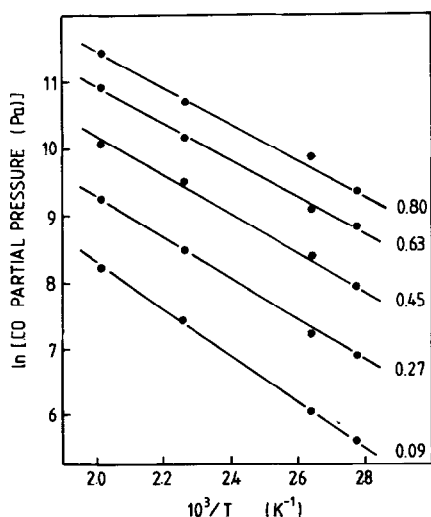


FIG. 6. Adsorption isosteres for CO on a reduced 4.1 wt% sample (2098–2104 cm⁻¹ band, Table 2) at constant absorbance. The numbers represent the surface coverage calculated as $\theta = A/A_{\infty 358}$ (see text).

tion with copper loading and therefore mean copper particle size (from 3 to 1 nm (16)) indicates an approximately uniform CO adsorption on very small particles. Given the curvatures in Fig. 7, it is clear that a Freundlich isotherm might approach the experimental data more closely, especially for the more highly loaded samples. For that situation

$$\Delta H_G = -\Delta H_m \ln \theta. \quad (2)$$

where ΔH_G is the enthalpy of adsorption at coverage θ and ΔH_m is a constant (37).

Plotting values of heats of adsorption from Fig. 2 according to Eq. (2) demonstrated an exponential decrease of ΔH_G with increasing θ (correlation coefficient >0.995) with the best estimates for ΔH_m being -1.8 kJ/mol (2.1 wt%), -3.2 kJ/mol (4.1 wt%), -5.6 kJ/mol (5.9 wt%), and -9.0 kJ/mol (9.5 wt%). These values are approximately proportional to the copper metal surface areas, and extrapolation to saturation surface coverage leads to a constant heat of adsorption (22 kJ/mol) for all catalysts used in this study.

3. CO Adsorption on Reduced Cu/SiO₂: Peak at 2175 cm⁻¹

In addition to the major peak due to CO adsorbed on the metallic component, Fig. 4 shows a much weaker absorption peak at 2175 ± 3 cm⁻¹, of half-width 38 ± 4 cm⁻¹ and of similar absorbance for each sample. This peak disappeared relatively rapidly when the cell was purged with either pure hydrogen or helium, while the peak near 2100 cm⁻¹ persisted about five times as long. Frequencies above that of gaseous CO (2143 cm⁻¹ (4)) have been reported by a few authors (12, 38) and are usually associated with weak adsorption on isolated species as mentioned above in the case of isolated Cu²⁺ ions. Gardner and Petrucci (38) have observed a weak band at 2173 cm⁻¹ which matches the broad shape described above. This frequency corresponds quite closely to that of gaseous CO⁺ (2184 cm⁻¹ (4)) which, in turn, might indicate a partial positive charge on the adsorption site (4).

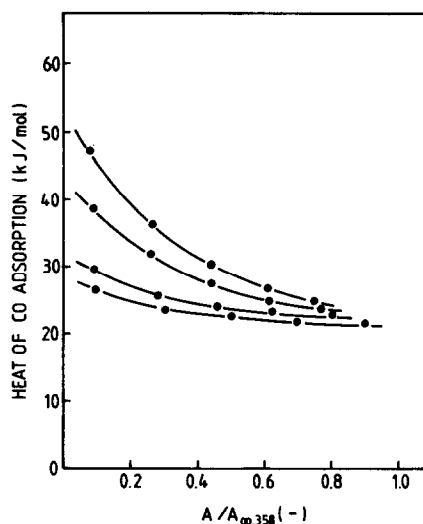


FIG. 7. Heat of adsorption of CO on metallic copper as a function of surface coverage $\theta = A/A_{\infty,358}$. From top to bottom, the samples are 9.5, 5.9, 4.1, and 2.1 wt% Cu/SiO₂.

The most reasonable assignment for the 2175 cm⁻¹ peak is to carbon monoxide bound to Cu⁺ sites distributed uniformly on the silica surface. These originate from copper ions exchanged with silanol groups and, when the support is the same, their absolute amount should be the same in each sample (15). Their valence state on reduction and constant quantity has been confirmed by XPS/AES measurements (16).

In view of the negligible fraction of surface covered by metallic copper particles (16), carbon monoxide adsorption on Cu⁺ is expected to be approximately equal for all samples, after adjustment for different disk weights. As seen from Fig. 8, no significant difference in normalized absorbance was detected for the four catalysts, except possibly slightly decreased values for higher copper loadings at substantial CO partial pressures (>15 kPa) (Fig. 8). The latter result would be consistent with some coverage of Cu⁺ sites by metallic copper particles at higher loadings, as expected from TEM analysis of the catalysts (16).

Plotting the data of Fig. 8 according to Eq. (1) gave parallel lines, giving the temperature-independent saturation absor-

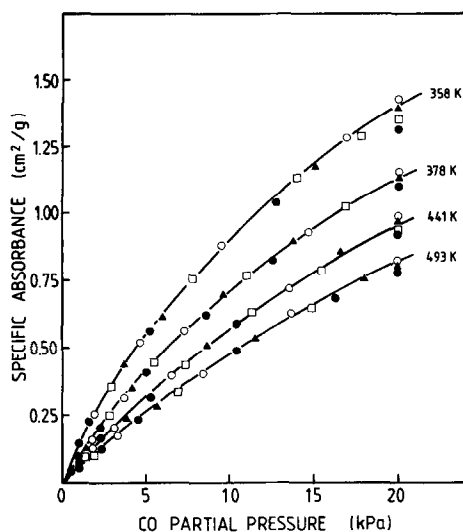


FIG. 8. Absorbance of CO adsorbed on isolated Cu⁺ (2175 cm⁻¹ band) at various temperatures after normalizing for the different catalyst disk weights. (○) 2.1 wt%, (▲) 4.1 wt%, (□) 5.9 wt%, and (●) 9.5 wt% Cu/SiO₂.

bances and adsorption equilibrium constants shown in Table 4. The Langmuir isotherm was fulfilled over the entire range of the study. The temperature dependence of the equilibrium constants indicated a heat adsorption on the isolated Cu⁺ sites of about 16 kJ/mol. The values for adsorption equilibrium constants for this adsorption were, roughly, 15 times smaller than those for CO adsorption on CuO particles (Table 1) and 4 to 10 times weaker than those for CO adsorption on the small Cu metal particles (Table 4). The data in Fig. 8 also allowed the calculation of adsorption isotherms at surface coverages up to 0.3: a constant heat of adsorption of 20 ± 1 kJ/mol was found this way. This low value is in agreement with the postulated weak adsorption and the results for the adsorption equilibrium constants described above.

4. CO Adsorption on Cu/SiO₂ Reoxidized in N₂O and Rereduction

It has been shown by XPS/AES analysis that partial reoxidation of reduced samples

in nitrous oxide at 450 K for 15 min converts Cu⁰ to Cu⁺ species alone and any further exposure at temperatures up to 520 K does not change this oxidation state (16). The reduced catalysts from the above were reoxidised at 500 K for 15 min and exposed to carbon monoxide sequentially at 358, 378, and 441 K. In accordance with earlier TPR results (16), partial rereduction was observed for all samples above approximately 420 K.

Features typical of oxidative interactions of Cu₂O with CO were again identified with peak intensities slightly smaller than those in the corresponding measurements on CuO. The characteristic frequencies of the two main peaks were shifted upwards by approximately 10 to 1528 cm⁻¹ (carbonates) and 1427 cm⁻¹ (bicarbonate) with the other characteristic bands remaining constant within ±5 cm⁻¹. The main feature attributed to carbon monoxide adsorption on the reoxidised samples is shown for adsorption at 358 K on all catalysts at approximate saturation coverage (>0.8) in Fig. 9. Under any experimental conditions of the study the minor absorption band around 2175 cm⁻¹ was indistinguishable from that attributed to carbon monoxide adsorption on isolated Cu⁺ species in the reduced sample although it is slightly less resolved from the major feature (compare Figs. 4 and 9). Given the sensitivity of the infrared technique to small differences in bonding it is concluded that the chemical state of this species is unaffected. This seems plausible

TABLE 4

Average Values for Normalised Absorbance at Saturation Coverage and Absorption Equilibrium Constants for Carbon Monoxide Adsorbed on Isolated Cu⁺ Species in Cu/SiO₂ Samples Reduced at 543 K

Temperature (K)	A _∞ (cm ² /g)	10 ⁵ × K (Pa ⁻¹)
358	3.2	4.7
378	3.1	3.6
441	3.1	2.2
493	3.0	1.4

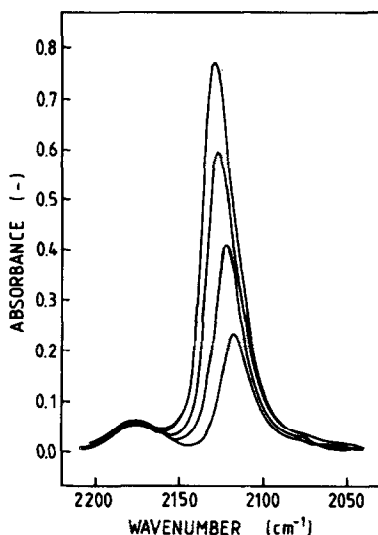


FIG. 9. CO adsorbed on catalysts reoxidised in N_2O at 20 kPa partial pressure (see text for details). The main infrared absorption band between 2118 and 2129 cm^{-1} is assigned to CO on bulk Cu crystals with the catalyst loading decreasing from top to bottom (9.5, 5.9, 4.1, and 2.1 wt%). The minor band around 2175 cm^{-1} is associated with CO on isolated Cu^+ sites as in Fig. 4.

on the basis of an independent copper species incorporated in the silica surface (16).

The major band was now centered around 2124 cm^{-1} , between those for adsorption on Cu^{2+} and Cu^0 forms. It can be attributed to carbon monoxide adsorbed on small Cu_2O clusters (5). When the surface coverage increased from 0.1 to saturation, a constant shift of 4–6 cm^{-1} towards higher frequencies was again observed for all catalysts, with the saturation maxima increasing as follows: 2119 cm^{-1} (2.1 wt%), 2122 cm^{-1} (4.1 wt%), 2127 cm^{-1} (5.9 wt%), and 2129 cm^{-1} (9.5 wt%). The half-width of the peaks remained constant at 20 ± 2 cm^{-1} . In the absence of any partial reduction (i.e., at 358 and 378 K), the adsorption data were closely represented by the Langmuir isotherm (Eq. 1) between 1.0 and 20 kPa.

During the complete reoxidation of Cu^0 particles to Cu^+ in nitrous oxide, small intraparticle rearrangement processes have

been identified for the copper clusters (16), as expressed by some particle regrowth towards the initial CuO size. The extent of this process is, however, small and the Cu_2O particles are only marginally bigger than the Cu metal clusters (16). Arguments similar to those above may therefore be applied to explain the shift of the saturation maxima with copper loading and the asymmetry of these absorption bands (Fig. 9), but these effects are expected to be less pronounced than those of metallic copper, as found experimentally.

Upon re-reduction of the partially oxidised samples in hydrogen (500 K, 30 min), spectra with characteristics typical of those shown in Figs. 4–7 and Tables 2 and 3 were reestablished on exposing the samples to CO/H_2 . This was true independently of the conditions of the preceding exposure to N_2O (temperature between 350 and 450 K, N_2O dilution from 100 to 1% in He). Unlike the case of fixed beds of catalyst used in the copper metal surface determination by N_2O decomposition (15, 39), where the considerable heat of reaction caused substantial catalyst modification (40), the thin disk of catalyst used in this study showed no such changes of structure. Rapid exposure of the reduced disk to air at temperatures as low as 298 K, however, caused almost complete loss of specific copper surface.

5. Extinction Coefficients of Different Copper Species

The samples used for the infrared measurements were much too small to enable determination of the absolute amount of CO adsorbed. Adsorption isotherms were measured volumetrically on a much larger sample (0.45 g) of the 5.9 wt% sample in unreduced, reduced, and reoxidised (in N_2O) forms. Crossplots against infrared absorbances at identical temperatures and CO pressures are shown in Fig. 10. The linearity is good and the slopes give the following extinction coefficients for the three forms of adsorbed CO:

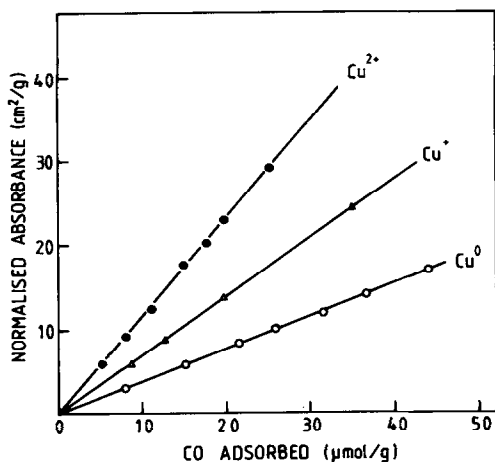


FIG. 10. Absorbance, normalised for disk weight, versus quantity of carbon monoxide adsorbed as obtained from volumetric measurements for 5.9% Cu/SiO₂ sample in calcined form (Cu²⁺), reduced form (Cu⁰) and following reoxidation in N₂O (Cu⁺).

Cu²⁺ (2127–2132 cm⁻¹):

$$\epsilon = 1.93 \times 10^{-18} \text{ cm}^2/\text{molecule}$$

Cu⁺ (2121–2126 cm⁻¹):

$$\epsilon = 1.20 \times 10^{-18} \text{ cm}^2/\text{molecule}$$

Cu⁰ (2103–2110 cm⁻¹):

$$\epsilon = 0.65 \times 10^{-18} \text{ cm}^2/\text{molecule.}$$

These values seem reasonable given the published data for CO adsorption on Pt (2.5×10^{-18} cm²/molecule (3, 24)) and Ru (0.44×10^{-18} cm²/molecule (3)). The values for Cu²⁺ and Cu⁺ correspond to adsorption on particles and it is unlikely they apply for adsorption on the corresponding isolated ions with their very different peak frequencies (2199 and 2175 cm⁻¹). This prevents assessment of the relative amounts of these species by spectroscopic means. However, on the basis of the saturation intensity (A_{∞}) for adsorption on metal clusters (bands around 2105 cm⁻¹, Table 4) and the copper metal surface areas measured by N₂O decomposition (15) assuming a copper surface density of 1.46×10^{19} atoms/m² (39), it was possible to calculate the Cu/CO atomic surface ratio for all catalysts under saturation

conditions (Table 5). The variation of the results with catalyst loading is probably not significant, although a slight increase of the ratio with increasing copper particle size may be detected. On the other hand, a substantial decrease of the saturation coverage with temperature is identified in accordance with earlier reports (33, 41). Saturation Cu/CO ratios of four have been found in several studies (42, 43) using low temperatures and low CO partial pressures. The results of this study also agree reasonably well with the results on Raney copper at 363 K (33). It is clear that with moderate pressures substantial amounts of carbon monoxide remain adsorbed on the Cu/SiO₂ catalysts even at temperatures above 450 K. Under catalytic conditions this can lead to rate inhibition (7, 34).

CONCLUSIONS

Infrared spectroscopy of adsorbed CO enables a definitive characterisation of Cu/SiO₂ catalysts prepared via the [Cu(NH₃)₄]²⁺ ion-exchange method (15) which is in excellent agreement with findings using a series of other techniques (16) and adds a number of interesting details. Two different copper species, identified as isolated atoms incorporated in the silica surface by ion exchange with two silanol groups and cluster copper agglomerated in particles of diameter below 5 nm, are revealed. The species have distinctly different properties for CO adsorption in the calcined, reduced, and reoxidised states.

TABLE 5

Ratio of Surface Copper Atoms to CO Molecules Adsorbed under Saturation Conditions, as Calculated from A_{∞} and the Measured Cu Metal Surface Areas (15)

Temperature (K)	Surface Cu/CO at saturation				
	2.1 wt%	4.1 wt%	5.9 wt%	9.5 wt%	Average
358	4.7	5.0	5.4	5.6	5.1
378	6.8	7.2	6.9	7.2	7.0
441	8.7	9.4	9.9	10.5	9.6
493	10.6	12.0	10.9	12.3	11.4

In the calcined catalysts, the two species are present as isolated Cu^{2+} ions and as CuO particles. Carbon monoxide adsorption on the former gives a weak band which is relatively less intense for samples of higher total copper loading. This is consistent with increasing coverage of the isolated species by extended CuO particles as the copper loading increases. Carbon monoxide adsorption on CuO particles is characterized by a constant heat of adsorption (29 kJ/mol) for all copper loadings and is independent of surface coverage. This indicates a uniformity of adsorption sites of this type, as expected from the flat-disk shape of the CuO particles observed by TEM (16).

Upon reduction, the isolated Cu^{2+} species reduce only as far as Cu^+ (16) and retain their isolated nature. Carbon monoxide adsorption on these sites is characterised by Langmuir adsorption with a heat of adsorption of 16–20 kJ mol⁻¹. The quantities adsorbed are similar for all four samples indicating little superposition of particulate copper on these sites. Carbon monoxide adsorption on the copper present as metal after reduction depends on particle size. For larger particles (~5 nm) the initial heat of adsorption approaches 50 kJ mol⁻¹ but declines steeply to 22 kJ mol⁻¹ with coverage. Peak frequencies, even at low coverage, exceed 2100 cm⁻¹ corresponding to adsorption on step structures possible on particles of this size. With small particles (<2 nm) heats of adsorption are relatively independent of coverage (20–30 kJ mol⁻¹). Peak frequencies are less than 2100 cm⁻¹ and characteristic of closely packed sites. The apparent saturation coverage of the metal by CO depends on temperature in the pressure range used and values between 5 (at 358 K) and 11 (at 493 K) Cu surface atoms per adsorbed CO molecule are inferred.

Reoxidation of samples with nitrous oxide at 500 K causes conversion of copper particles to the Cu(I) cuprous oxide state. Adsorption of CO is then characterised by infrared frequencies and intensities inter-

mediate between those observed for the corresponding Cu(II) and Cu(0) states.

ACKNOWLEDGMENTS

Financial support by the National Energy Research Development and Demonstration Program and the Australian Research Grants Scheme is gratefully acknowledged. One of us (Marc Kohler) was partially supported by a grant under the joint CSIRO-Macquarie University scheme. The Aerosil catalyst supports were kindly supplied by Degussa Australia Pty. Ltd.

REFERENCES

1. Eischens, R. P., and Pliskin, W. A., in *Advances in Catalysis and Related Subjects* (D. D. Eley, W. G. Frankenburg, V. I. Komaretsky, and P. B. Weisz, Eds.), Vol. 10, p. 1. Academic Press, New York, 1958.
2. Eischens, R. P., *Acc. Chem. Res.* **5**, 74 (1972).
3. Miura, H., and Gonzalez, R. D., *J. Phys. E.* **15**, 373 (1982).
4. London, J. W., and Bell, A. T., *J. Catal.* **31**, 32 (1973).
5. London, J. W., and Bell, A. T., *J. Catal.* **31**, 96 (1973).
6. De Jong, K. P., Geus, J. W., and Joziassse, J., *Appl. Surf. Sci.* **6**, 273 (1980).
7. Monti, D. M., Cant, N. W., Trimm, D. L. and Wainwright, M. S., *J. Catal.* **100**, 17 (1986).
8. Pritchard, J., *J. Vac. Sci. Technol.* **9**, 895 (1972).
9. Pritchard, J., Catterick, T., and Gupta, R. K., *Surf. Sci.* **53**, 1 (1975).
10. Pritchard, J., Catterick, T., and Gupta, R. K., *Surf. Sci.* **54**, 1 (1976).
11. Horn, K. and Pritchard, J., *Surf. Sci.* **55**, 701 (1976).
12. De Jong, K. P., Geus, J. W., and Joziassse, J., *J. Catal.* **65**, 437 (1980).
13. Davydov, A. A., Rubene, N. A., and Budneva, A. A., *Kinet. Katal.* **19**, 776 (1978).
14. Smith, A. W., and Quets, J. M., *J. Catal.* **4**, 163 (1965).
15. Kohler, M. A., Lee, J. C., Trimm, D. L., Cant, N. W., and Wainwright, M. S., *Appl. Catal.* **31**, 309 (1987).
16. Kohler, M. A., Curry-Hyde, H. E., Hughes, A. E., Sexton, B. A., and Cant, N. W., *J. Catal.* **108**, 323 (1987).
17. Sundquist, B. E., *Acta Metall.* **12**, 67 (1964).
18. McLean, M., *Acta Metall.* **19**, 387 (1971).
19. Baiker, A., and Holstein, W. L., *J. Catal.* **84**, 178 (1983).
20. Seanor, D. A., and Amberg, C. H., *J. Chem. Phys.* **42**, 2967 (1965).
21. Boccuzzi, F., Ghiotti, G., and Chiorino, A., *Surf. Sci.* **156**, 933 (1985).

22. Bocuzzi, F., Ghiotti, G., and Chiorino, A., *Surf. Sci.* **162**, 361 (1985).
23. Sexton, B. A., *Surf. Sci.* **88**, 391 (1979).
24. Little, L. H., "Infrared Spectra of Adsorbed Species," Academic Press, New York/London, 1966.
25. Chesters, M. A., and Pritchard, J., *Surf. Sci.* **28**, 460 (1971).
26. Crossley, A., and King, D. A., *Surf. Sci.* **68**, 528 (1977).
27. Moskovits, M., and Hulse, J. E., *Surf. Sci.* **78**, 397 (1978).
28. Stoop, F., Toolenaar, F. J. C. M., and Ponec, V., *J. Catal.* **73**, 50 (1982).
29. Toolenaar, F. J. C. M., Stoop, F., and Ponec, V., *J. Catal.* **82**, 1 (1983).
30. Kavtaradze, N. N., and Sokolov, N. P., *J. Phys. Chem.* **44**, 603 (1970).
31. O'Neill, C. E., and Yates, D. J. C., *J. Phys. Chem.* **65**, 901 (1965).
32. Sheppard, N., and Nguyen, T. T., "Advances in Infrared and Raman Spectroscopy" (R. J. H. Clark and R. E. Hester, Eds.), Vol. 5. Heyden, London, 1978.
33. Wainwright, M. S., "Proceedings, Int. Congress on Alcohol Fuels, Sydney, 1978," Session 8, p. 1. Institution Chemical Engineers, NSW Group, 1978.
34. Monti, D. M., Wainwright, M. S., Trimm, D. L., and Cant, N. W., *Ind. Eng. Chem. Prod. Res. Dev.* **24**, 397 (1985).
35. Tracy, J. C., *J. Chem. Phys.* **56**, 2478 (1972).
36. Papp, H., and Pritchard, J., *Surf. Sci.* **53**, 371 (1975).
37. Halsey, G. D., *Adv. Catal.* **4**, 259 (1952).
38. Gardner, R. A., and Petrucci, R. H., *J. Amer. Chem. Soc.* **82**, 5051 (1960).
39. Evans, J. W., Wainwright, M. S., Bridgewater, A. J., and Young, D. J., *Appl. Catal.* **7**, 75 (1983).
40. Giamello, E., Fubini, B., Lauro, P., and Bossi, A., *J. Catal.* **87**, 443 (1984).
41. Dalmon, J. A., and Martin, G. A., *J. Catal.* **66**, 214 (1980).
42. Moskovits, M., and Hulse, J. E., *Surf. Sci.* **61**, 302 (1976).
43. Bond, G. C., and Turnham, B. D., *J. Catal.* **45**, 128 (1976).